Development and optimization of *N*-acetylneuraminic acid biosensors in *Bacillus subtilis*

Xiaolong Zhang[a, b], Yanting Cao[a, b], Yanfeng Liu[a, b*], Long Liu[a, b], Jianghua Li[b], Guocheng Du[a, b], Jian Chen[b, c*]

[a]Key Laboratory of Carbohydrate Chemistry and Biotechnology, Ministry of Education, Jiangnan University, Wuxi 214122, China

[b]Key Laboratory of Industrial Biotechnology, Ministry of Education, Jiangnan University, Wuxi 214122, China

[c]National Engineering Laboratory for Cereal Fermentation Technology, Jiangnan University, Wuxi 214122, China

*Corresponding authors:

Yanfeng Liu

Tel.: +86-510-85197117, Fax: +86-510-85918309, E-mail: yanfengliu@jiangnan.edu.cn

Jian Chen

Tel.: +86-510-85913661, Fax: +86-510-85910799, E-mail: jchen@jiangnan.edu.cn

This article has been accepted for publication and undergone full peer review but has not been through the copyediting, typesetting, pagination and proofreading process, which may lead to differences between this version and the Version of Record. Please cite this article as doi: 10.1002/bab.1942.

Abstract

Transcriptional factor (TF)-based metabolite-responsive biosensors are important tools for screening engineered enzymes with desired properties and for the dynamic regulation of biosynthetic pathways. However, TF-based biosensor construction is often constrained by undesired effects of TF-binding site sequence insertion on gene expression and unpredictable optimal TF expression levels. In the present study, a stepwise TF-based biosensor construction approach was developed using an N-acetylneuraminic acid (NeuAc) biosensor for *Bacillus subtilis,* as a case study. Specifically, 12 promoters with various strengths were selected as the first promoter library. Next, binding site sequences for the NanR were inserted into various positions of the selected promoter sequences to develop the second promoter library, resulting in 6 engineered promoters containing TF-binding site sequences (NanO), without major effects on promoter strength. NanR expression cassettes with different expression levels were further integrated to construct the biosensor library, yielding 9 NeuAc biosensors with efficient repression in the absence of NeuAc. Finally, biosensor activation was characterized by testing fold changes in expression levels of the green fluorescent protein reporter in the presence of NeuAc *in vivo*, which revealed 61-fold activation when NeuAc was present. The NeuAc biosensor developed in this study can be used for screening engineered enzymes for enhanced NeuAc biosynthesis in *B. subtilis*.

Keywords

N-acetylneuraminic acid, transcriptional factor-based biosensor, *Bacillus subtilis*

Highlights:

1. *N*-acetylneuraminic acid biosensors in *Bacillus subtilis* were developed and optimized.

2. The optimal NeuAc biosensor revealed 61-fold activation when NeuAc was present.

3. This biosensor can be potentially used for metabolic regulation and directed evolution of key enzymes for NeuAc biosynthesis in *B. subtilis*.

Introduction

With the increasing demand for sustainable development with low carbon emission, the application of synthetic biology-driven cell factories for chemical biomanufacturing has been shown to be advantageous. This technique has shown promise for the production of chemicals and pharmaceuticals such as the industrial intermediate 1,3-propylene glycol; the pharmaceutical intermediate artemisinic acid; and the nutraceuticals *N*-acetylglucosamine (GlcNAc) and human milk oligosaccharide [1–8]. Biosensor-based dynamic regulation and high-throughput screening technologies are important applications of synthetic biology. In particular, metabolite-responsive biosensors can be divided into riboswitch-based biosensors and transcriptional factor (TF)-based biosensors, according to the regulatory mechanism utilized. Compared to riboswitch-based biosensors, TF-based biosensors have wider application owing the large number of metabolite-binding TFs identified. Successful applications of TF-based biosensors include fatty acid/acyl-CoA biosensors that regulate the activation of synthetic pathways to increase the yield of fatty acid ethyl ester and the high-throughput

optimization of genetic regulatory elements of metabolic pathways to improve the synthesis efficiency of target products [4].

Although biosensors have great prospects for screening engineered enzymes to enhance target product biosynthesis and the dynamic regulation of biosynthetic pathways, the development and utilization of biosensors still face many challenges. First, TF binding site sequence insertion often causes adverse and unpredictable effects on promoter activity [5, 6]. Second, it is difficult to predict the optimal TF binding site sequence insertion position and copy number, which limits the efficiency of the construction and application of TF-based metabolite-responsive biosensors. [7–9]. Third, biosensors require cross-species optimization, because they are often found in non-target production hosts, that further increases the difficulty of biosensor optimization due to the need to change the promoter and optimize the expression levels [10].

N-acetylneuraminic acid (NeuAc) is one of the major sialic acids. It is a monomer of sialylated human milk oligosaccharide and can promote infant brain development, maintain brain health, and enhance immunity [11]. In the present study, a stepwise TF-based biosensor was designed and developed. This strategy was then validated by building a NeuAc biosensor in *Bacillus subtilis* (*B. subtilis).* (Fig. 1). First, based on literature mining, 12 promoters with different expression intensities were rationally selected for the first promoter library. The binding sequence of the NanR, derived from *Escherichia coli* (*E. coli*), was then inserted into each promoter sequence in various positions, to develop a second promoter library. Engineered promoters without a major reduction in promoter strength after inserting the NanR binding sequence were selected. Further, NanR expression cassettes with different expression levels were inserted into the selected promoters to obtain biosensors with effective inhibition of gene expression in the absence of NeuAc. Finally, the activation of the

NeuAc biosensor was tested by adding NeuAc to the culture medium and by using NeuAc-producing *B. subtilis*. The stepwise TF-based biosensor construction approach and the NeuAc biosensor developed in this study can potentially be used for the construction of other TF-based metabolite-responsive biosensors. Moreover, the optimal NeuAc biosensor constructed in this study may be used for screening engineered enzymes and the dynamic regulation of metabolic pathways to enhance NeuAc biosynthesis in *B. subtilis*.

2. Materials and Methods

2.1. Microorganisms and cultivation conditions

B. subtilis 168 and BGPD-YtsJ-2 (NeuAc synthetic pathway strain, constructed in a previous study) were used in this study [12]. The BGPD-YtsJ-2 strain was cultured at 50 °C for 24 h to eliminate the NeuAc synthesis pathway plasmid, and then was transformed with the veg105-nanR6k biosensor plasmid to obtain the BSB strain. The BGPD-YtsJ-2 strain was transformed with the veg105-nanR6k biosensor plasmid to obtain the BSANB strain. p7Z6P43, p7S6P43, p7C6P43, and pHT01 plasmids were used from preparations stored in our laboratory.

E. coli was cultured in Luria-Bertani broth and on agar plates. *B. subtilis* was cultured in fermentation medium (pH 7.0), containing 12 g/L yeast extract, 6 g/L peptone, 6 g/L $(NH_4)_2SO_4$, 12.5 g/L $K_2HPO_4{\cdot}4H_2O$, 2.5 g/L KH_2PO_4, 3 g/L $MgSO_4{\cdot}7H_2O$, and 44 g/L glucose.

The *B. subtilis* strains were inoculated in a 24-well plate, containing 1.5 mL of fermentation medium and maintained at 37 °C, with shaking at 220 rpm.

2.2. Plasmid construction

All constructed plasmids are listed in Table 1. Promoters were amplified from *B. subtilis* 168 [19] and the green fluorescent protein (GFP) gene was amplified from a template plasmid previously constructed in our laboratory. They were then inserted into the pHT01 plasmid using the ClonExpress II One Step Cloning Kit (Vazyme, Nanjing, China) to obtain the first promoter library of 12 plasmids. The second promoter library was obtained by reverse amplification polymerase chain reaction (PCR) using the first promoter library as a template (Supplementary Fig. 1 to Fig. 9). The *gerBC*, *ydjO*, *lytE*, and *veg* promoters were amplified from *B. subtilis*[19] and the NanR binding site was amplified from *E. coli*. They were then inserted into the second promoter library using the ClonExpress II One Step Cloning Kit, to obtain the third promoter library.

2.3. NeuAc transport pathway construction

The NeuAc transport pathway construction primers are listed in Supplementary Table 1. The recombination fragment was obtained by overlap extension-PCR and transformed into *B. subtilis* strains using a previously described method [13]. The following antibiotics were used for selection: 30 μg/mL kanamycin, 50 μg/mL spectinomycin, 60 μg/mL zeocin, and 5 μg/mL chloramphenicol. The NeuAc transporter genes, *nanT* and *nan*C, from *E. coli* MG1655 were integrated into the genome of the original *B. subtilis* 168 strain, yielding the strains BSnanT and BSnanC. The BSnanCT strain, overexpressing both *nanC* and *nanT*, was also constructed.

2.4. Analytical methods

GlcNAc, ManNAc, and NeuAc were analyzed by high-performance liquid chromatography (HPLC) (Agilent 1200 series; Agilent, Santa Clara, CA, USA) using an Aminex HPX-87H column (300 × 7.8 mm) with UV detection (210 nm). The mobile phase was 10 mM H_2SO_4, at a flow rate of 0.5 mL/min. The retention times of NeuAc, ManNAc, and GlcNAc were 9.5, 13.0, and 13.6 min, respectively.

Cells were harvested by centrifugation at 8,000 × g for 10 min. Extraction solution (2 mL; acetonitrile: methanol:water = 4:4:2) was then added to the cells and they were incubated at 4 °C overnight. After freeze-drying, 0.5 mL of water was added to obtain samples for determining GlcNAc, ManNAc, and NeuAc concentrations by HPLC.

To determine the GFP yield, 0.2 mL of fermentation broth (48 h) was added to each well of a 96-well black plate (#3603; Corning Inc, Corning, NY, USA). Fluorescence intensity and cell optical density were determined using a multi-mode microplate reader (Cytation 3; Biotek, Winooski, VT, USA). The relative fluorescence intensity of GFP was measured at an excitation wavelength of 490 nm, an emission wavelength of 530 nm, and a gain value of 60. Cell optical density was determined at a wavelength of 600 nm [14]. Activation intensity was defined as the expression intensity of GFP activation when 5 g/L NeuAc was added to the medium. Leakage intensity was defined as the intensity of GFP expression without the addition of NeuAc. Activation and leakage intensity were calculated using the following equations:

activation intensity = $(GFP_1/OD_{600\text{-}1}\text{-}GFP_2/OD_{600\text{-}2})/(GFP_3/OD_{600\text{-}3}\text{-}GFP_4/OD_{600\text{-}4})$ and

leakage intensity = $(GFP_3/OD_{600\text{-}3}\text{-}GFP_4/OD_{600\text{-}4})/(GFP_1/OD_{600\text{-}1}\text{-}GFP_2/OD_{600\text{-}2})$,

where GFP_1 and $OD_{600\text{-}1}$ are the fluorescence intensity and OD_{600} of *B. subtilis* harboring the biosensor plasmid, respectively, when 5 g/L NeuAc was added externally; GFP_2 and $OD_{600\text{-}2}$ are the fluorescence intensity and OD_{600} of *B. subtilis* without the biosensor plasmid, respectively, when 5 g/L NeuAc was added externally; GFP_3 and $OD_{600\text{-}3}$ are the fluorescence intensity and OD_{600} of *B. subtilis* harboring the biosensor plasmid, respectively, when 0 g/L NeuAc was added externally; and GFP_4 and $OD_{600\text{-}4}$ are the fluorescence intensity and OD_{600} of *B. subtilis* without the biosensor plasmid, respectively, when 0 g/L NeuAc was added externally. Triplicate experiments were performed in *B. subtilis*.

The folding energy of the promoters was calculated using the NUPACK web server (http://www.nupack.org/). The mRNA sequence used for folding energy calculation was from +1 of the promoter to the first 50 base pairs of the GFP sequence.

3. Results

3.1 NeuAc biosensor library design

The natural NeuAc biosensor was based on NanR-mediated regulation from *E. coli*, which activates the expression of the NeuAc degradation pathway genes in the presence of NeuAc, via the release of the repressor protein, NanR, from binding sequences in the vicinity of NeuAc degradation pathway gene promoters [15]. In a previous study, Kalivoda et al. analyzed the binding mechanism of NanR and determined that the binding sequence of NanR is ttnannTGGTATAACAGGTATAnAGnTAnnnnnTnn, where uppercase bases are immutable sequences, the lowercase bases are variable sequences, and “n” is any base [16]. Peters et al. optimized the

function of a NeuAc biosensor in *E. coli* based on this regulatory mechanism of NanR [17]. However, the construction and application of NeuAc biosensors in microorganisms that are generally recognized as safe (GRAS), such as *B. subtilis*, is still lacking.

Promoter library engineering is an effective strategy for designing a biosensor. For example, the sort-seq strategy based on fluorescence-activated cell sorting and high-throughput sequencing can efficiently elucidate unknown interaction mechanisms of transcriptional factors and their target DNA sequences, which can be used to guide biosensor construction [18]. Because the regulatory mechanism of NanR and its DNA binding sequences has previously been reported, this information can be directly used to guide NeuAc biosensor construction. In order to construct and optimize a NeuAc biosensor efficiently and conveniently, we designed a construction strategy based on three rounds of promoter library selection and engineering. First, we selected 12 promoters with 25-fold intensity differences, originating from *hbs*, *odhA*, *asd*, *srfAA*, *gltX*, *veg*, *citZ*, *yceC*, *phrE*, *csbA*, *sigH*, and *yvyD* genes, to control GFP expression. This was the first promoter library for NeuAc biosensor construction (Supplementary Fig. 1)[14]. The NanR binding sequence was then inserted into different positions of the 12 promoters (in the vicinity of -35 box, -10 box, and ribosome binding site sequences) to construct the second promoter library. Finally, promoters with the desired levels of GFP expression after insertion of the NanR binding sequence were selected from the second library to further combine the repressor protein, NanR, at four different expression levels to construct the NeuAc biosensor library. This strategy allowed for the screening of biosensors with both high activation levels and the desired expression levels.

3.2 Effects of inserting NanR binding sequence in promoters on expression level

The construction of artificially induced promoters is usually performed based on the semi-rational design of the modular combination of promoter elements [19]. Therefore, the second promoter library of the NeuAc biosensors was constructed based on the semi-rational design approach, aiming to optimize the variable and arbitrary base sequences of the NanR binding sequence and inserting NanR binding sequences into the optimal position within the selected promoters, while ensuring that the core sequence of the promoter was not altered (-35 and -10 box). The specific integration promoter sequence and folding energy are shown in supplementary Figures 2 to 9 and supplementary table 2.

Most of the constructed promoters lost their ability to drive gene expression after insertion of the NanR binding sequences. Only 16 promoters, namely veg104, veg105, odhA352, hbs103, gltX351, gltX105, gltX106, srfAA105, citZ351, citZ352, citZ104, citZ105, yvyD104, csbA101, csbA102, and yveC102, maintained their original expression levels (Fig. 2). In particular, the veg105, srfAA105, citZ351, odhA352, citZ104, and hbs104 promoters among the 16 promoters showed a minimum decrease in activity. In particular, the veg- and citZ-series promoters showed greater robustness after the insertion of the NanR binding sequence in the -10 region, indicating that these two promoters are more inclusive in this region. The veg104 and veg105 promoters had the highest activity in the second promoter library (fluorescence intensity of GFP around 24,000 arbitrary units [a.u.] and 20,000 a.u., respectively), which was less than 20% lower than the activity of the *veg* promoter. Notably, the hbs103 promoter showed increased GFP expression levels from approximately 11,000 to 24,000 a.u. after the integration of the NanR binding sequence. The inserted NanR binding sequence

may have positive effects on promoter structure and thus increases the transcriptional activity of promoter P_{hbs}.

3.3 Construction and validation of NeuAc biosensor library with different NanR expression levels

Regulating protein expression levels is one of the most important factors in biosensor construction and optimization processes. If the expression levels are too low, there may not be any regulatory effects, while if they are too high, it may cause protein anabolic stress to the cells and affect endogenous physiological metabolism [20, 21]. Based on the 16 integrated promoters selected from the second promoter library, 6 promoters, namely veg105, srfAA105, citZ351, odhA352, citZ104, and hbs104, which showed a minimum decrease in activity, were selected to further insert an expression cassette for the repressor protein, NanR, under the control of promoters with different activities. This resulted in the construction of the third library (relative fluorescent intensity: gerBC, 1,800 a u.; ydjO, 6,000 a.u.; lytE, 8,000 a u.; veg, 12,000 a.u.) [14].

We found that the effects of NanR expression levels on the 6 different promoters tested were not identical (Fig. 3). The biosensor based on veg105 and srfAA105 showed a cliff-like repression of expression when the expression levels of NanR were greater than 6000 a.u., while citz351, odhA352, and citz104 showed a gradient repression of expression, inversely correlated with NanR expression levels. To minimize the burden of NanR expression on cellular metabolism, the intensity of NanR expression should be kept as low as possible, while still achieving regulatory functions. Therefore, veg105-nanR6k and srfAA105-nanR8k were selected for biosensor testing.

3.4 Evaluation of the constructed biosensors by exogenous addition of NeuAc and endogenous NeuAc synthesis

The NeuAc biosensor was able to down-regulate gene expression by NanR regulatory proteins in the absence of NeuAc. *B. subtilis* cannot transfer NeuAc intracellularly to activate NeuAc biosensor (Supplementary Fig. 10). To further verify whether it can be activated by NeuAc, we first constructed a *B. subtilis* strain expressing the NeuAc transporters NanC and NanT from *E. coli* and tested the effects of exogenous NeuAc on GFP expression levels (pH 7.0, adjusted by sodium hydroxide). *B. subtilis* strains BS168-nanT, BS168-nanC, and BS168-nanCT, with expression cassettes for NanT, NanC, or both NanT and NanC, respectively, under the control of the P_{43} promoter integrated into the genome, were constructed. Extracellular NeuAc (5 g/L) can be successfully transported and activate GFP expression when NanT or NanC is overexpressed. However, by an unknown mechanism, the activation of GFP expression was severely affected when NanT and NanC were co-overexpressed (Fig. 4a, 4b and 4c). Therefore, the BS168-nanT strain was selected as the host for validation of the NeuAc biosensor, due the smaller effect of NanT overexpression on the growth of this strain.

A total of 9 biosensors, namely veg105-nanR6k, veg105-nanR8k, srfAA105-nanR6k, srfAA105-nanR8k, srfAA105-nanR12k, citz351-nanR12k, odhA352-nanR12k, hbs104-nanR8k, and hbs104-nanR12k, were tested in the BS168-nanT strain, with 5 g/L NeuAc added to the culture medium. The biosensors, veg105-nanR6k, veg105-nanR8k, srfAA105-nanR6k, and srfAA105-nanR8k were found to be activated to drive GFP expression by NeuAc addition (Fig. 4d). In particular, the veg105-nanR6k biosensor showed optimal properties, with an

activation intensity of 4000 a.u. and only 4% leakage expression. Furthermore, we re-integrated a NanR binding sequence in the -10 region, to obtain veg1052-nanR6k and srfAA1052-nanR8k biosensors, based on the veg105-6k and srfAA105-nanR8k biosensors, respectively. The activation intensity of the srfAA1052-nanR8k biosensor decreased by more than 50% compared with that of the control, indicating that the addition of NanR binding sequence had a greater effect on the srfAA105 promoter. The activation intensity of the veg1052-nanR6k biosensor decreased by approximately 20%, but it had a 61-fold higher activation intensity, with only 1.6% leakage, when NeuAc was absent (Fig. 4e). Although we obtained a NeuAc biosensor with a relatively low level of expression leakage, further efforts are required to reduce the expression leakage levels and obtain a significant improvement in the signal-to-noise output ratio. Further optimization of the RNA polymerase binding site and the transcription factor binding site through promoter engineering are required to improve the biosensor [22]. To more accurately determine the characteristics of the NeuAc biosensor, we added NeuAc to the medium at 0 to 5.0 g/L and continuously measured GFP expression for 42 h. The biosensor was shown to have a two-step activation, firstly at 0 to 0.1 g/L NeuAc and then at 2 to 3 g/L NeuAc. This was also observed for biosensor srfAA105-nanR8k and requires further investigation (Fig. 5a and Supplementary Fig. 11). In particular, the veg105-nanR6k biosensor was rapidly activated within 3 h when 5 g/L NeuAc was added to the medium (Fig. 5b). This rapid activation of the biosensor to control gene expression has important applications in metabolic engineering and synthetic biology.

Finally, the BGPD-YtsJ-2 strain was cultured at 50 °C for 24 h to eliminate the NeuAc synthesis pathway plasmid, and then was transformed with the veg105-nanR6k biosensor plasmid to obtain the BSB strain, and found that it was not activated. We transformed the veg105-nanR6k biosensor into the BGPD-YtsJ-2 strain

(containing the NeuAc synthetic pathway with 2.18 g/L NeuAc production) to obtain BSANB strain, and found that it was efficiently activated at 24 and 48 h (Fig. 5c). In particular, we found that the expression level of the veg105-nanR6k biosensor in NeuAc-producing strains was much higher than in those that required exogenous NeuAc addition. However, the production of extracellular NeuAc (2.18 g/L) in the BSANB strain was lower than that after the addition of exogenous NeuAc at 5 g/L. This implied that the NanT transporter from *E. coli* did not efficiently transport extracellular NeuAc into *B. subtilis*. In addition, the intracellular NeuAc concentration of NeuAc-producing strain BSANB was low (Fig. 5d), which indicated that the NeuAc biosensor can be activated by very small amounts of NeuAc. This is consistent with the activation of the NeuAc biosensor by 0.1 g/L exogenous NeuAc. Although NeuAc added about 3 g/L of NeuAc, NeuAc biosensor can show gradient changes. However, because the lower concentration of NeuAc in the NeuAc-producing strain can activate the NeuAc biosensor, it may only be suitable for the initial screening process of enzyme-directed evolution to remove the inactive mutants. If an accurate gradient response is required to achieve the goal of directed evolution screening, it is necessary to further design a production strain that matches the NeuAc biosensor response range.

4. Conclusions

TF-based biosensors are widely used as important tools for high-throughput screening of engineered enzymes and strains and the dynamic regulation of metabolic pathways. In this study, a stepwise TF-based biosensor was constructed, based on the selection of various promoter strengths, TF binding sequence insertion and optimization, TF expression level optimization, and *in vivo* biosensor activation testing. This

strategy will allow for the screening of biosensors with both high levels of gene expression activation and the desired expression levels. Based on the approach described here, a NeuAc biosensor with a 61-fold activation of gene expression in the presence of NeuAc was constructed in *B. subtilis*. This biosensor can potentially be used for metabolic regulation and the directed evolution of key enzymes for NeuAc biosynthesis in *B. subtilis*.

5. Acknowledgements

Not applicable.

6. Declarations of interest

The authors declare that they have no competing financial interests.

7. Author contributions

Xiaolong Zhang and Yanting Cao contributed equally to this work. Yanfeng Liu, Long Liu, Jianghua Li, Guocheng Du, and Jian Chen designed the experiments. Xiaolong Zhang and Yanting Cao performed the experiments. Yanfeng Liu, Long Liu, Jianghua Li, Guocheng Du, and Jian Chen conceived the project. Xiaolong Zhang, Yanting Cao, and Yanfeng Liu analyzed the data and wrote the paper.

8. Funding

This work was financially supported by the National Key Research and Development Program of China (2018YFA0900300), the National Natural Science Foundation of China (31972854, 31622001, 31671845, 21676119), the Key Research and Development Program of Jiangsu Province (BE2019628), the 111 Project (No. 111-2-06), and the National First-Class Discipline Program of Light Industry Technology and Engineering (LITE2018-16).

9. References

[1] Jullesson D, David F, Pfleger B, Nielsen J. (2015). Impact of synthetic biology and metabolic engineering on industrial production of fine chemicals. *Biotechnology advances*. **33:** 1395–1402.

[2] Jong B de, Siewers V, Nielsen J. (2012). Systems biology of yeast: enabling technology for development of cell factories for production of advanced biofuels. *Current opinion in biotechnology*. **23:** 624–630.

[3] van Dijl J, Hecker M. (2013). Bacillus subtilis: from soil bacterium to super-secreting cell factory. *Microbial Cell Factories*. **12:** 3.

[4] J Andrew Jones, Ö Duhan Toparlak, Mattheos AG Koffas. (2015). Metabolic pathway balancing and its role in the production of biofuels and chemicals. *Current opinion in biotechnology*. **33:** 52–59.

[5] Zhang J, Jensen M, Keasling J. (2015). Development of biosensors and their application in metabolic engineering. *Current Opinion in Chemical Biology*. **28:** 1–8.

[6] Zhang F, Keasling J. (2011). Biosensors and their applications in microbial metabolic engineering. *Trends in Microbiology*. **19:** 323–329.

[7] Sanvicens N, Mannelli I, Salvador J-P, Valera E, Marco M-P. (2011). Biosensors for pharmaceuticals based on novel technology. *TrAC Trends in Analytical Chemistry*. **30:** 541–553.

[8] Rogers J, Taylor N, Church G. (2016). Biosensor-based engineering of biosynthetic pathways. *Current opinion in biotechnology*. **42:** 84–91.

[9] Eggeling L, Bott M, Marienhagen J. (2015). Novel screening methods—biosensors. *Current opinion in biotechnology*. **35:** 30–36.

[10] Paepe BD, Peters G, Coussement P, Maertens J, Mey MD. (2017). Tailor-made transcriptional biosensors for optimizing microbial cell factories. *J Ind Microbiol Biotechnol*. **44:** 623–645.

[11] Zhang X, Liu Y, Liu L, Li J, Du G, Chen J. (2019). Microbial production of sialic acid and sialylated human milk oligosaccharides: Advances and perspectives. *Biotechnology advances*.

[12] Zhang X, Liu Y, Liu L, Wang M, Li J, Du G, Chen J. (2018). Modular pathway engineering of key carbon-precursor supply-pathways for improved N-acetylneuraminic acid production in Bacillus subtilis. *Biotechnol Bioeng*. **115:** 2217–2231.

[13] Zhang X-Z, Zhang Y-H. (2011). Simple, fast and high-efficiency transformation system for directed evolution of cellulase in Bacillus subtilis. *Microbial biotechnology*. **4:** 98–105.

[14] Yang S, Du G, Chen J, Kang Z. (2017). Characterization and application of endogenous phase-dependent promoters in Bacillus subtilis. *Appl Microbiol Biotechnol*. **101:** 4151–4161.

[15] Kalivoda K, Steenbergen S, Vimr E. (2013). Control of the Escherichia coli sialoregulon by transcriptional repressor NanR. *J Bacteriol*. **195:** 4689–4701.

[16] Kathryn A. Kalivoda, Susan M. Steenbergen, Eric R. Vimr, and Jacqueline Plumbridge. (2013). Regulation of Sialic Acid Catabolism by the DNA Binding Protein. *J Bacteriol*. **185:** 4806–4815.

[17] Peters G, Paepe B de, Wannemaeker L de, Duchi D, Maertens J, Lammertyn J, Mey M de. (2018). Development of N-acetylneuraminic acid responsive biosensors based on the transcriptional regulator NanR. *Biotechnol Bioeng*. **115:** 1855–1865.

[18] Rohlhill J, Sandoval N, Papoutsakis E. (2017). Sort-Seq Approach to Engineering a Formaldehyde-Inducible Promoter for Dynamically Regulated Escherichia coli Growth on Methanol. *ACS Synth Biol*. **6:** 1584–1595.

[19] Stanton B, Nielsen A, Tamsir A, Clancy K, Peterson T, Voigt C. (2014). Genomic mining of prokaryotic repressors for orthogonal logic gates. *Nature chemical biology*. **10:** 99.

[20] Liu Y, Liu Y, Wang M. (2017). Design, optimization and application of small molecule biosensor in metabolic engineering. *Frontiers in microbiology*. **8:** 2012.

[21] Park M, Tsai S-L, Chen W. (2013). Microbial biosensors: engineered microorganisms as the sensing machinery. *Sensors*. **13:** 5777–5795.

[22] Chen S-Y, Wei W, Yin B-C, Tong Y, Lu J, Ye B-C. (2019). Development of a Highly Sensitive Whole-Cell Biosensor for Arsenite Detection through Engineered Promoter Modifications. *ACS Synth Biol*. **8:** 2295–2302.

Figures legend

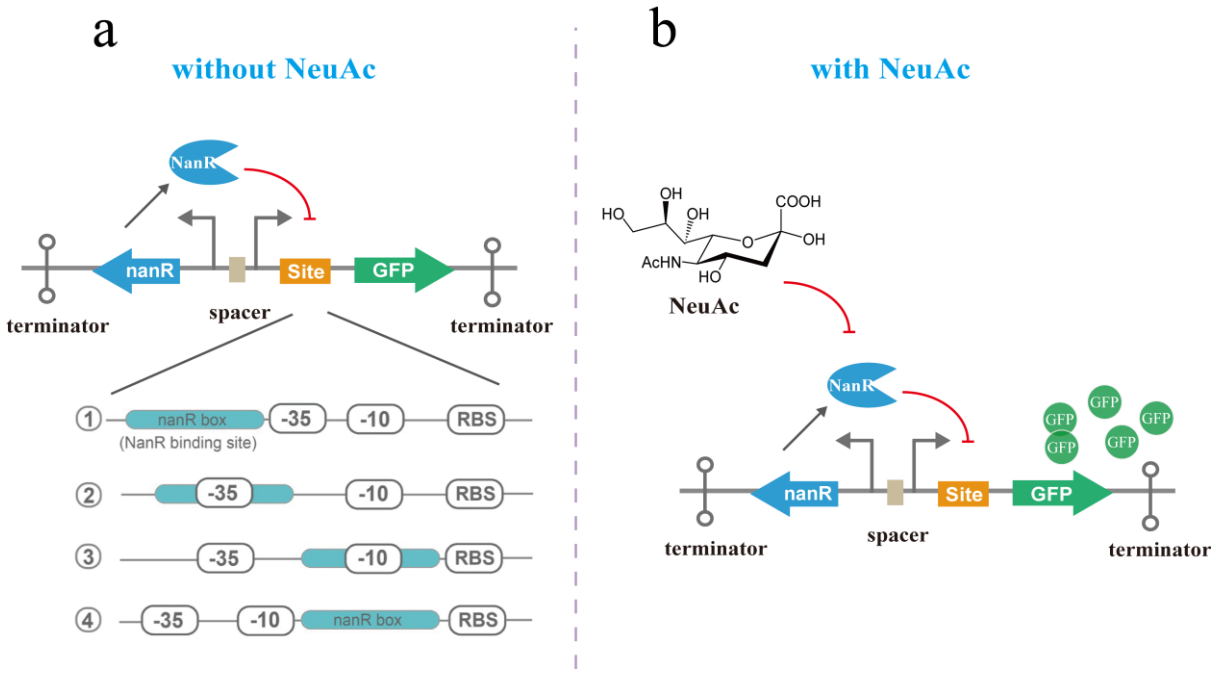

Fig. 1. Schematic of NeuAc biosensor structure. (a) The function of the NeuAc biosensor when NeuAc is absent. When NeuAc is absent, the constitutively expressed NanR binds to the binding sequence (site) to inhibit GFP expression. (b) The function of the NeuAc biosensor when NeuAc is present. When NeuAc is present, NeuAc binds to NanR to activate GFP expression.

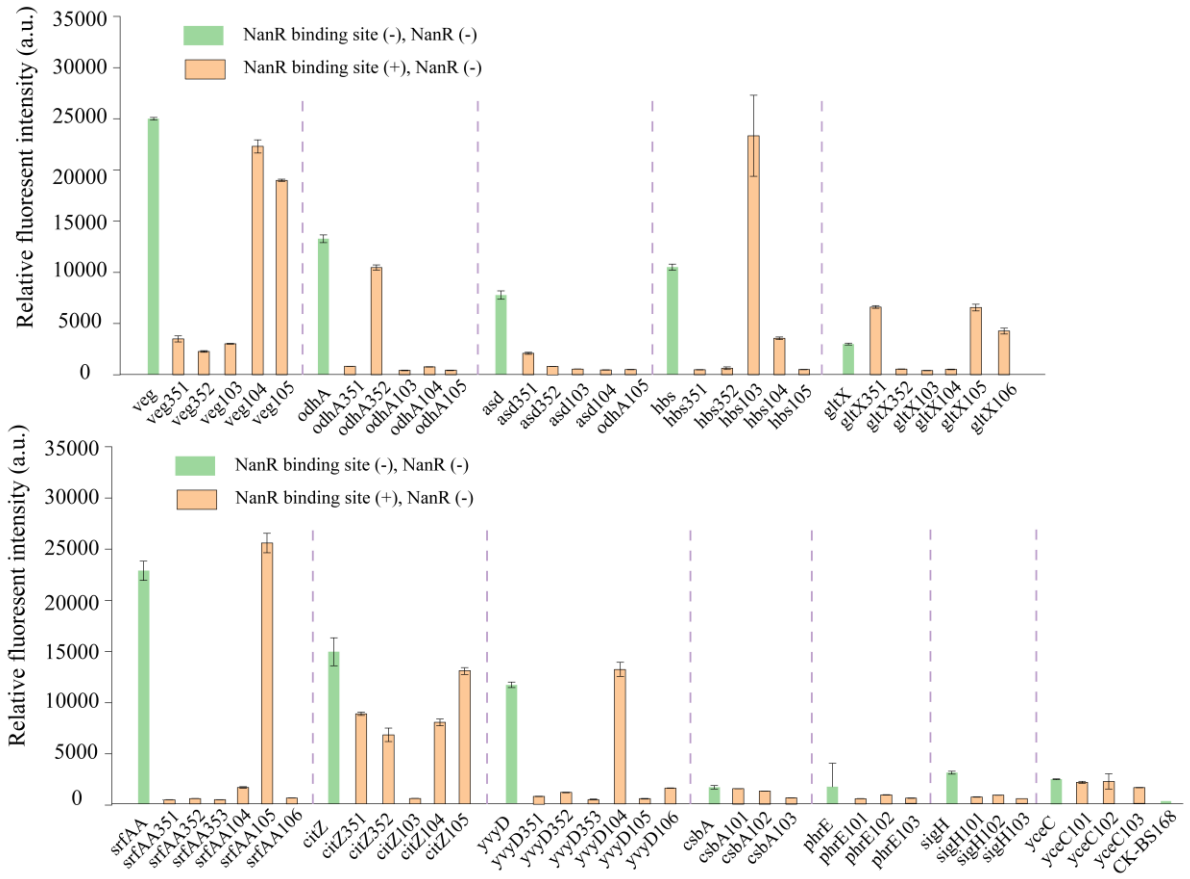

Fig. 2. Effects of inserting the NanR binding sequence on promoter strength. The NanR binding sequence was inserted into different positions of the 12 promoters (in the vicinity of the -35 box, -10 box, and ribosome binding site sequences) to construct the second NeuAc biosensor library. Engineered promoter strength was tested using GFP as a reporter. Triplicate experiments were performed in *B. subtilis* and error bars represent the standard deviation.

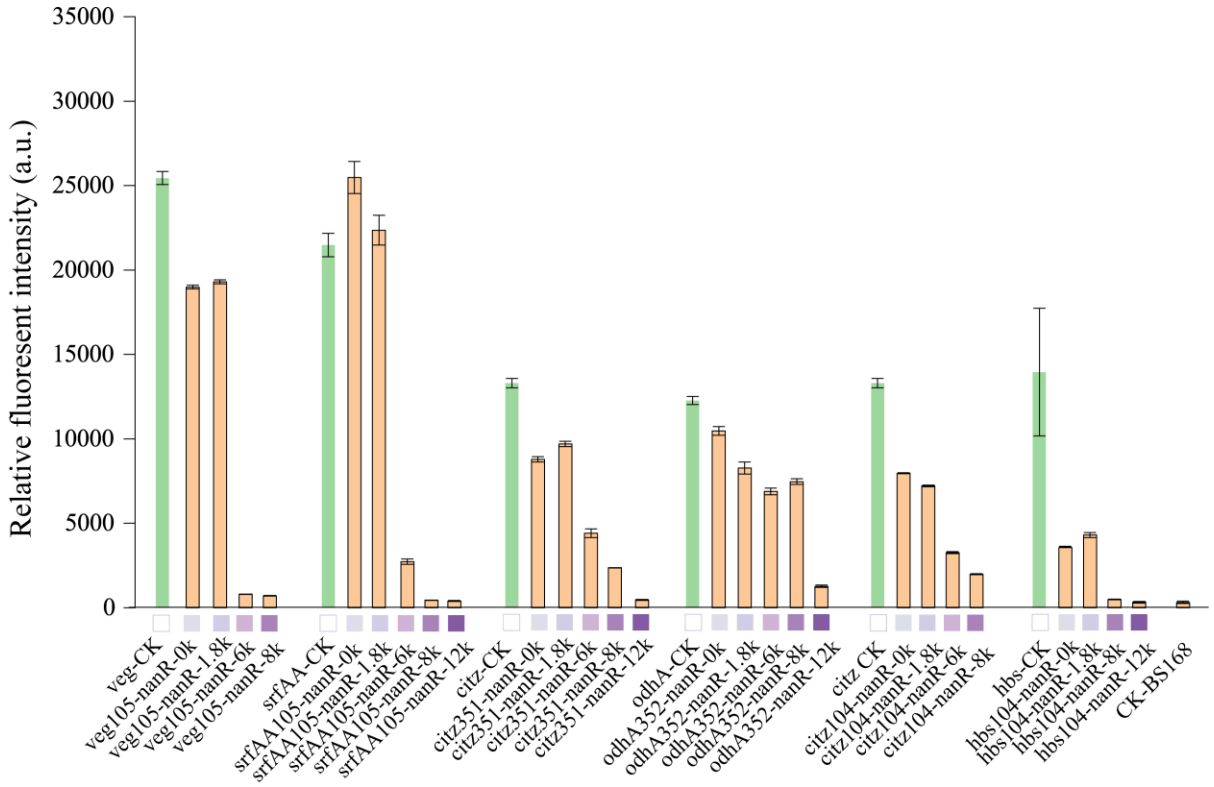

Fig. 3. Effects of NanR expression on the strength of promoters engineered with NanR binding sequence insertion. The promoter with stable GFP expression after the insertion of the NanR binding sequence was selected from the second library to further express the repressor protein, NanR, at four different levels to construct the third NeuAc biosensor library. Triplicate experiments were performed in *B. subtilis* and error bars represent the standard deviation.

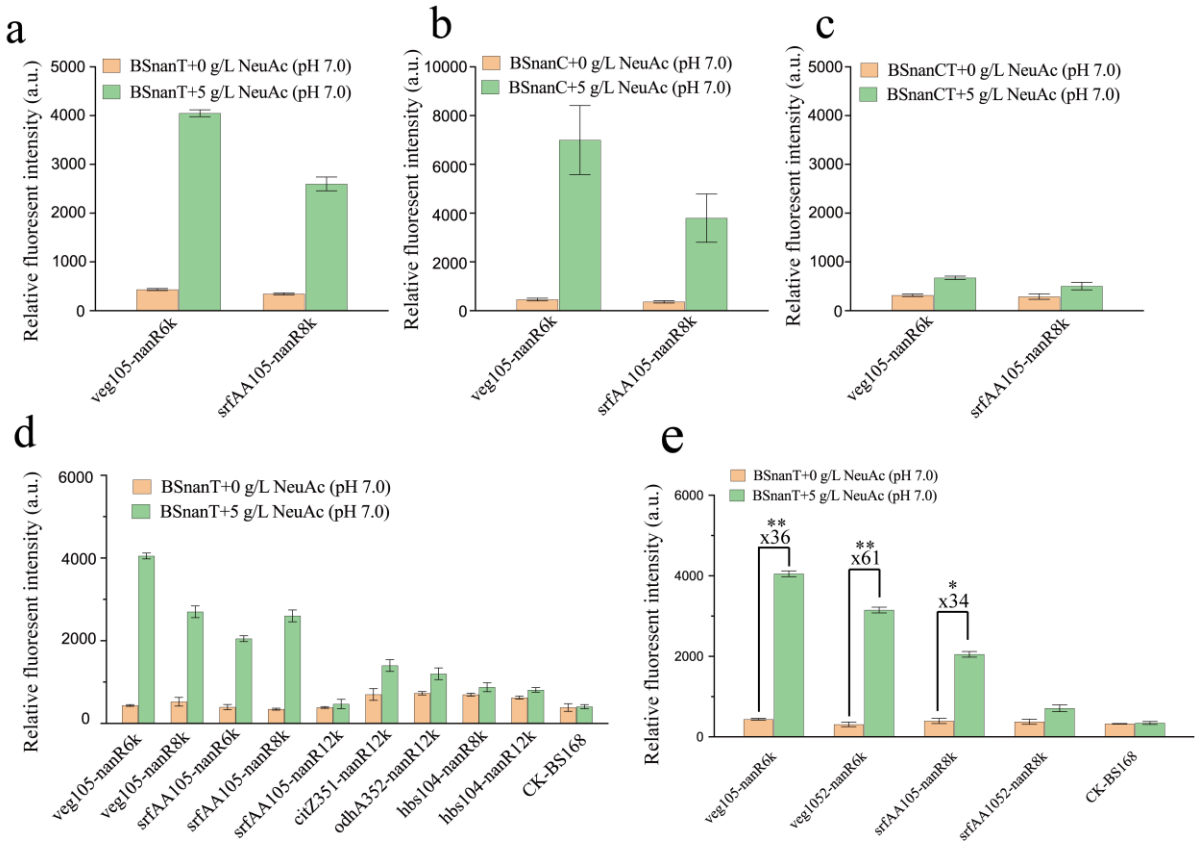

Fig. 4. NeuAc biosensor testing after the addition of 5 g/L exogenous NeuAc. (a) Evaluation of the NeuAc transporter, NanT, from *E. coli* in *B. subtilis* by testing GFP expression levels under the control of veg105-nanR6k and srfAA105-nanR8k biosensors in *B. subtilis* with NanT expression. (b) Evaluation of the NeuAc transporter, NanC, from *E. coli* in *B. subtilis* by testing GFP expression levels under the control of veg105-nanR6k and srfAA105-nanR8k biosensors in *B. subtilis* with NanC expression. (c) Evaluation of the effects of co-expression of the NeuAc transporters, NanT and NanC, from *E. coli* on transporting NeuAc in *B. subtilis* by testing GFP expression levels under the control of veg105-nanR6k and srfAA105-nanR8k biosensors in *B. subtilis* with NanT and NanC co-expression. (d) The characteristics of the third NeuAc biosensor library were determined in the BSnanT strain. (e) A further increase of one copy of the NanR binding sequence in the promoter reduced the leakage level of the NeuAc biosensor. *$p < 0.05$, ** $p < 0.01$

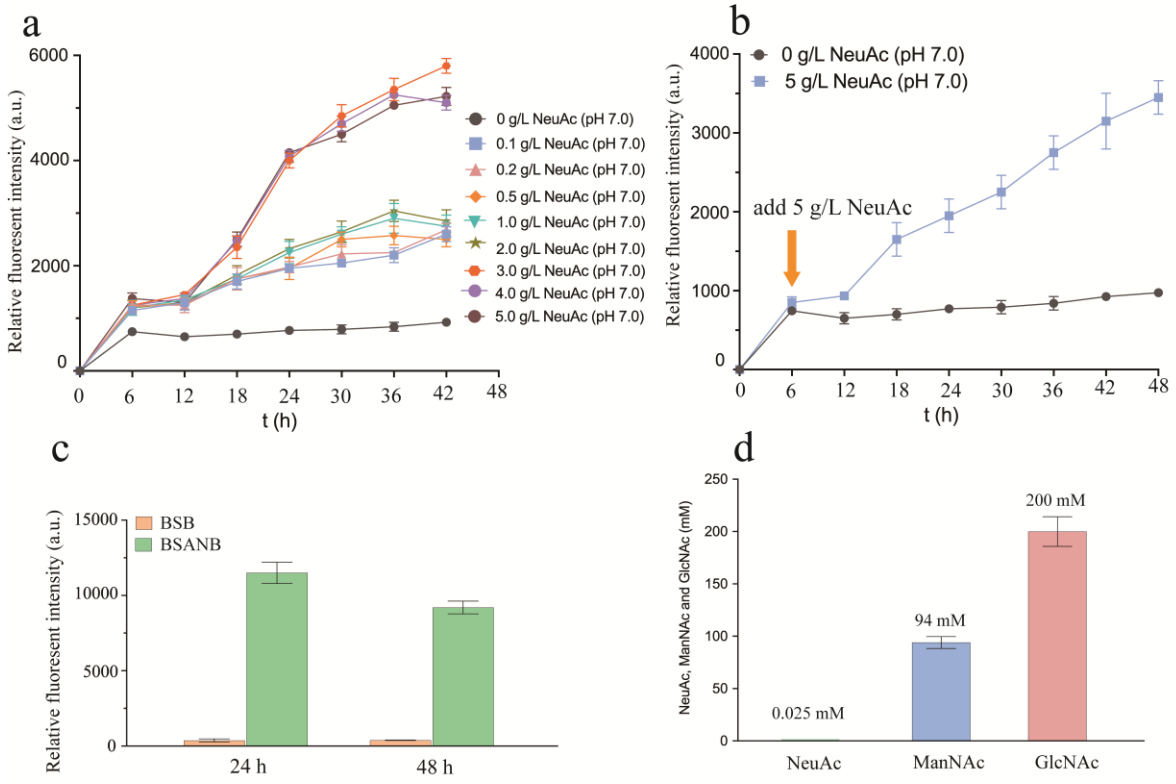

Fig. 5. Characterization of the veg105-nanR6k biosensor response to various NeuAc concentrations and verification of the functionality of the veg105-nanR6k biosensor in NeuAc-producing *B. subtilis*. (a) NeuAc was added to the culture medium (t = 0 h) at 0, 0.1, 0.2, 0.5, 1.0, 2.0, 3.0, 4.0, or 5.0 g/L to determine the activation curve of the veg105-nanR6k biosensor. (b) The veg105-nanR6k biosensor activation curve was verified by adding 5 g/L NeuAc at 6 h. (c) The veg105-nanR6k biosensor was evaluated in BSB and BSANB strains. The BSB strain does not contain NeuAc synthetic pathway plasmid, but contains the veg105-nanR6k biosensor plasmid. The BSANB strain contains the NeuAc synthetic pathway plasmid and the veg105-nanR6k biosensor plasmid. (d) Intracellular NeuAc content of the NeuAc-producing strain at 48 h.

Table legend

Table 1 Strains and plasmids used in this study.

Table 1 Strains and plasmids used in this study

Names	Characteristics	Reference
Strains		
BGPD-YtsJ-2	*B. subtilis* 168 derivate, contains NeuAc synthesis pathway	[12]
BSB	BGPD-YtsJ-2 derivate, cultured 24 h at 50°C to eliminate the NeuAc synthesis pathway plasmid, and then was transformed with the veg105-nanR6k biosensor plasmid.	This work
BSANB	BGPD-YtsJ-2 derivate, contains the veg105-nanR6k biosensor plasmid.	This work
BSnanT	*Bacillus subtilis* 168 derivate, overexpression of *nanT* under the control of promoter P_{43}	This work
BSnanC	*Bacillus subtilis* 168 derivate, overexpression of *nanC* under the control of promoter P_{43}	This work
BsnanCT	*Bacillus subtilis* 168 derivate, overexpression of *nanT* and *nanC* under the control of promoter P_{43}	This work
Plasmid		
P7Z6P43	P7Z6 containing P_{43} promoter	[12]
P7S6P43	P7S6 containing P_{43} promoter	[12]
P7C6P43	P7C6 containing P_{43} promoter	[12]
pHT-hbs-GFP	pHT01 containing P_{hbs} and GFP	This work
pHT-ohdA-GFP	pHT01 containing P_{ohdA} and GFP	This work

pHT-asd-GFP	pHT01 containing P_{asd} and GFP	This work
pHT-srfAA-GFP	pHT01 containing P_{srfAA} and GFP	This work
pHT-gltX-GFP	pHT01 containing P_{gltX} and GFP	This work
pHT-veg-GFP	pHT01 containing P_{veg} and GFP	This work
pHT-citz-GFP	pHT01 containing P_{citz} and GFP	This work
pHT-yceC-GFP	pHT01 containing P_{yceC} and GFP	This work
pHT-phrE-GFP	pHT01 containing $P_{phrE}$and GFP	This work
pHT-csbA-GFP	pHT01 containing P_{csbA} and GFP	This work
pHT-sigH-GFP	pHT01 containing P_{sigH} and GFP	This work
pHT-yvyD-GFP	pHT01 containing P_{yvyD} and GFP	This work
pHT-veg351	Integration of NanR recognition sequences near the P_{veg} promoter -35 region	This work
pHT-veg352	Integration of NanR recognition sequences near the P_{veg} promoter -35 region	This work
pHT-veg103	Integration of NanR recognition sequences near the P_{veg} promoter -10 region	This work
pHT-veg104	Integration of NanR recognition sequences near the P_{veg} promoter -10 region	This work
pHT-veg105	Integration of NanR recognition sequences near the P_{veg} promoter -10 region	This work

pHT-odhA351	Integration of NanR recognition sequences near the P_{odhA} promoter -35 region	This work
pHT-odhA352	Integration of NanR recognition sequences near the P_{odhA} promoter -35 region	This work
pHT-odhA103	Integration of NanR recognition sequences near the P_{odhA} promoter -10 region	This work
pHT-odhA104	Integration of NanR recognition sequences near the P_{odhA} promoter -10 region	This work
pHT-odhA105	Integration of NanR recognition sequences near the P_{odhA} promoter -10 region	This work
pHT-asd351	Integration of NanR recognition sequences near the P_{asd} promoter -35 region	This work
pHT-asd352	Integration of NanR recognition sequences near the P_{asd} promoter -35 region	This work
pHT-asd103	Integration of NanR recognition sequences near the P_{asd} promoter -10 region	This work
pHT-asd104	Integration of NanR recognition sequences near the P_{asd} promoter -10 region	This work
pHT-asd105	Integration of NanR recognition sequences near the P_{asd} promoter -10 region	This work
pHT-hbs351	Integration of NanR recognition sequences near the P_{hbs} promoter -35 region	This work

pHT-hbs352	Integration of NanR recognition sequences near the P_{hbs} promoter -35 region	This work
pHT-hbs353	Integration of NanR recognition sequences near the P_{hbs} promoter -35 region	This work
pHT-hbs104	Integration of NanR recognition sequences near the P_{hbs} promoter -10 region	This work
pHT-hbs105	Integration of NanR recognition sequences near the P_{hbs} promoter -10 region	This work
pHT-gltX351	Integration of NanR recognition sequences near the P_{gltX} promoter -35 region	This work
pHT-gltX352	Integration of NanR recognition sequences near the P_{gltX} promoter -35 region	This work
pHT-gltX103	Integration of NanR recognition sequences near the P_{gltX} promoter -10 region	This work
pHT-gltX104	Integration of NanR recognition sequences near the P_{gltX} promoter -10 region	This work
pHT-gltX105	Integration of NanR recognition sequences near the P_{gltX} promoter -10 region	This work
pHT-gltX106	Integration of NanR recognition sequences near the P_{gltX} promoter -10 region	This work
pHT-srfAA351	Integration of NanR recognition sequences near the P_{srfAA} promoter -35 region	This work

pHT-srfAA352	Integration of NanR recognition sequences near the P_{srfAA} promoter -35 region	This work
pHT-srfAA353	Integration of NanR recognition sequences near the P_{srfAA} promoter -35 region	This work
pHT-srfAA104	Integration of NanR recognition sequences near the P_{srfAA} promoter -10 region	This work
pHT-srfAA105	Integration of NanR recognition sequences near the P_{srfAA} promoter -10 region	This work
pHT-srfAA106	Integration of NanR recognition sequences near the P_{srfAA} promoter -10 region	This work
pHT-citZ351	Integration of NanR recognition sequences near the P_{citZ} promoter -35 region	This work
pHT-citZ352	Integration of NanR recognition sequences near the P_{citZ} promoter -35 region	This work
pHT-citZ103	Integration of NanR recognition sequences near the P_{citZ} promoter -10 region	This work
pHT-citZ104	Integration of NanR recognition sequences near the P_{citZ} promoter -10 region	This work
pHT-citZ105	Integration of NanR recognition sequences near the P_{citZ} promoter -10 region	This work
pHT-yvyD351	Integration of NanR recognition sequences near the P_{yvyD} promoter -35 region	This work

pHT-yvyD352	Integration of NanR recognition sequences near the P_{yvyD} promoter -35 region	This work
pHT-yvyD353	Integration of NanR recognition sequences near the P_{yvyD} promoter -35 region	This work
pHT-yvyD104	Integration of NanR recognition sequences near the P_{yvyD} promoter -10 region	This work
pHT-yvyD105	Integration of NanR recognition sequences near the P_{yvyD} promoter -10 region	This work
pHT-yvyD106	Integration of NanR recognition sequences near the P_{yvyD} promoter -10 region	This work
pHT-csbA101	Integration of NanR recognition sequences near the P_{csbA} promoter -10 region	This work
pHT-csbA102	Integration of NanR recognition sequences near the P_{csbA} promoter -10 region	This work
pHT-csbA103	Integration of NanR recognition sequences near the P_{csbA} promoter -10 region	This work
pHT-phrE101	Integration of NanR recognition sequences near the P_{phrE} promoter -10 region	This work
pHT-phrE102	Integration of NanR recognition sequences near the P_{phrE} promoter -10 region	This work
pHT-phrE103	Integration of NanR recognition sequences near the P_{phrE} promoter -10 region	This work

pHT-sigH101	Integration of NanR recognition sequences near the P_{sigH} promoter -10 region	This work
pHT-sigH102	Integration of NanR recognition sequences near the P_{sigH} promoter -10 region	This work
pHT-sigH103	Integration of NanR recognition sequences near the P_{sigH} promoter -10 region	This work
pHT-yceC101	Integration of NanR recognition sequences near the P_{yceC} promoter -10 region	This work
pHT-yceC102	Integration of NanR recognition sequences near the P_{yceC} promoter -10 region	This work
pHT-yceC103	Integration of NanR recognition sequences near the P_{yceC} promoter -10 region	This work
pHT-veg105-nanR1.8k	Expression of transcriptional regulatory protein NanR by P_{gerBC} promoter (1800 a. u.) in pHT-veg105	This work
pHT-veg105-nanR6k	Expression of transcriptional regulatory protein NanR by P_{lytE} promoter (6000a. u.) in pHT-veg105	This work
pHT-veg105-nanR8k	Expression of transcriptional regulatory protein NanR by P_{ydjO} promoter (8000 a. u.) in pHT-veg105	This work
pHT-srfAA105-nanR1.8k	Expression of transcriptional regulatory protein NanR by P_{gerBC} promoter (1800 a. u.) in pHT-srfAA105	This work
pHT-srfAA105-nanR6k	Expression of transcriptional regulatory protein NanR by P_{lytE} promoter (6000a. u.) in pHT-srfAA105	This work

pHT-srfAA105-nanR8k	Expression of transcriptional regulatory protein NanR by P_{ydjO} promoter (8000 a. u.) in pHT-srfAA105	This work
pHT-srfAA105-nanR12k	Expression of transcriptional regulatory protein NanR by P_{veg} promoter (12000 a. u.) in pHT-srfAA105	This work
pHT-citz351-nanR1.8k	Expression of transcriptional regulatory protein NanR by P_{gerBC} promoter (1800 a. u.) in pHT-citz351	This work
pHT-citz351-nanR6k	Expression of transcriptional regulatory protein NanR by P_{lytE} promoter (6000a. u.) in pHT-citz351	This work
pHT-citz351-nanR8k	Expression of transcriptional regulatory protein NanR by P_{ydjO} promoter (8000 a. u.) in pHT-citz351	This work
pHT-citz351-nanR12k	Expression of transcriptional regulatory protein NanR by P_{veg} promoter (12000 a. u.) in pHT-citz351	This work
pHT-odhA352-nanR1.8k	Expression of transcriptional regulatory protein NanR by P_{gerBC} promoter (1800 a. u.) in pHT-odhA352	This work
pHT-odhA352-nanR6k	Expression of transcriptional regulatory protein NanR by P_{lytE} promoter (6000a. u.) in pHT-odhA352	This work
pHT-odhA352-nanR8k	Expression of transcriptional regulatory protein NanR by P_{ydjO} promoter (8000 a. u.) in pHT-odhA352	This work
pHT-odhA352-nanR12k	Expression of transcriptional regulatory protein NanR by P_{veg} promoter (12000 a. u.) in pHT-odhA352	This work
pHT-citZ104-nanR1.8k	Expression of transcriptional regulatory protein NanR by P_{gerBC} promoter (1800 a. u.) in pHT-citZ104	This work

pHT-citZ104-nanR6k	Expression of transcriptional regulatory protein NanR by P_{lytE} promoter (6000a. u.) in pHT-citZ104	This work
pHT-citZ104-nanR8k	Expression of transcriptional regulatory protein NanR by P_{ydjO} promoter (8000 a. u.) in pHT-citZ104	This work
pHT-citZ104-nanR12k	Expression of transcriptional regulatory protein NanR by P_{veg} promoter (12000 a. u.) in pHT-citZ104	This work
pHT-hbs104-nanR1.8k	Expression of transcriptional regulatory protein NanR by P_{gerBC} promoter (1800 a. u.) in pHT-hbs104	This work
pHT-hbs104-nanR6k	Expression of transcriptional regulatory protein NanR by P_{lytE} promoter (6000a. u.) in pHT-hbs104	This work
pHT-hbs104-nanR8k	Expression of transcriptional regulatory protein NanR by P_{ydjO} promoter (8000 a. u.) in pHT-hbs104	This work
pHT-hbs104-nanR12k	Expression of transcriptional regulatory protein NanR by P_{veg} promoter (12000 a. u.) in pHT-hbs104	This work
pHT-veg1052-nanR6k	Add 1 copy of NanR recognition sequence to pHT-veg105-nanR6k	This work

Graphical Abstract

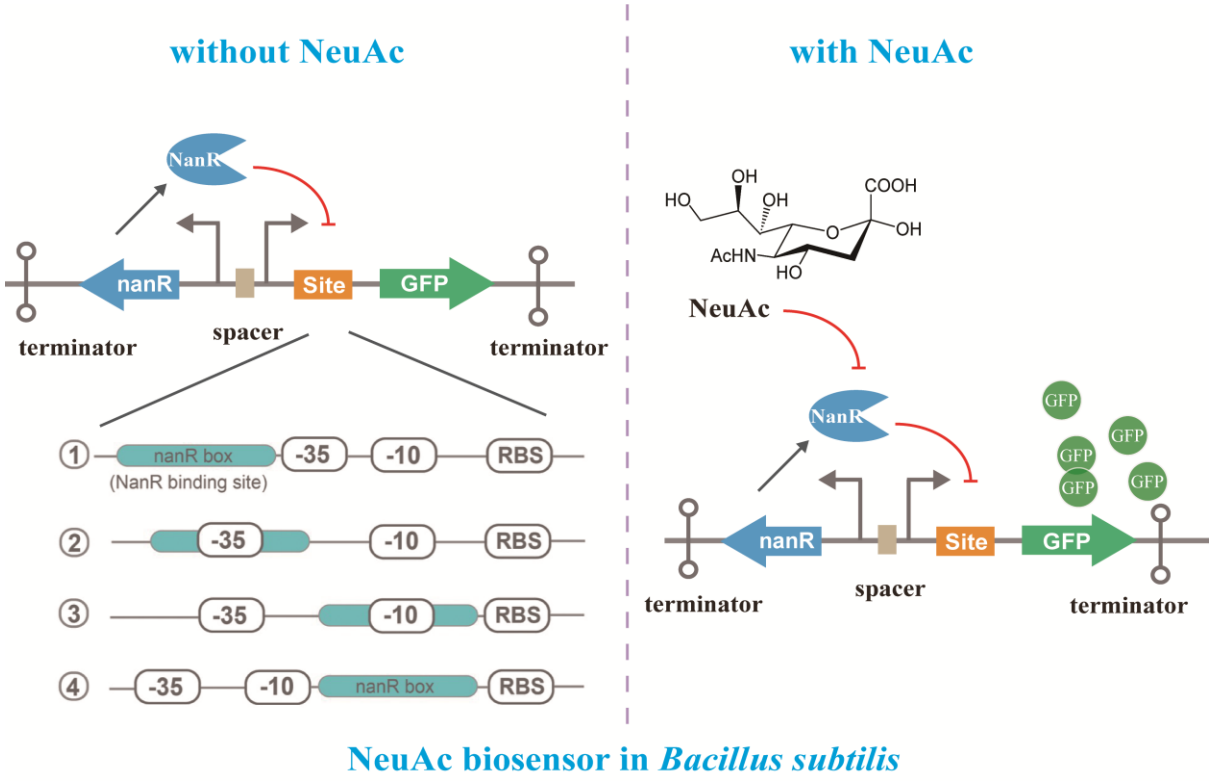

NeuAc biosensor in *Bacillus subtilis*